MIXED HYBRID FINITE ELEMENT EDDINGTON ACCELERATION OF DISCRETE ORDINATES SOURCE ITERATION

February 20, 2017

Samuel S. Olivier
Texas A&M University
Department of Nuclear Engineering
smsolivier@tamu.edu

Introduction

One of the most challenging computational tasks is simulating the interaction of radiation with matter. A full description of a particle in flight includes three spatial variables (x,y and z), two angular or direction of flight variables (μ = the cosine of the polar angle and γ = the azimuthal angle), one energy variable (E) and one time variable (t). Numerical solutions require discretizing all seven variables leading to immense systems of algebraic equations. In addition, material properties can lead to vastly different solution behaviors making generalized numerical methods for radiation transport difficult to attain [1].

Lawrence Livermore National Laboratory (LLNL) is developing a high–order radiation–hydrodynamics code. The hydrodynamics portion is discretized using the Mixed Hybrid Finite Element Method (MHFEM), where values are taken to be constant within a cell with discontinuous jumps at both cell edges [2]. MHFEM is particularly suited for hydrodynamics but not for radiation transport. This work seeks to develop an acceleration scheme capable of robustly reducing the number of iterations in Discrete Ordinates Source Iteration calculations while being compatible with MHFEM multiphysics.

Background

The steady–state, mono–energetic, isotropically–scattering, fixed–source Linear Boltzmann Equation in planar geometry is:

$$\mu\frac{\partial\psi}{\partial x}(x,\mu)+\Sigma_t(x)\psi(x,\mu)=\frac{\Sigma_s(x)}{2}\int_{-1}^{1}\psi(x,\mu')d\mu'+\frac{Q(x)}{2} \tag{1}$$

where $\mu=\cos\theta$ is the cosine of the angle of flight θ relative to the x–axis, $\Sigma_t(x)$ and $\Sigma_s(x)$ the total and scattering macroscopic cross sections, $Q(x)$ the isotropic fixed–source and $\psi(x,\mu)$ the angular flux [1]. This is an integro–differential equation due to the placement of the unknown, $\psi(x,\mu)$, under both a derivative and integral.

The Discrete Ordinates (S_N) angular discretization sets μ to discrete values stipulated by an N–point Gauss quadrature rule. The scalar flux, $\phi(x)$, is then

$$\phi(x)=\int_{-1}^{1}\psi(x,\mu)\,\mathrm{d}\mu\xrightarrow{S_N}\sum_{n=1}^{N}w_n\psi_n(x) \tag{2}$$

where $\psi_n(x)=\psi(x,\mu_n)$ and w_n are the quadrature weights corresponding to each μ_n [3]. The S_N equations are then

$$\mu_n\frac{\mathrm{d}\psi_n}{\mathrm{d}x}(x)+\Sigma_t(x)\psi_n(x)=\frac{\Sigma_s(x)}{2}\phi(x)+\frac{Q(x)}{2},\ 1\le n\le N \tag{3}$$

where $\phi(x)$ is defined by Eq. 2. This is now a system of N coupled, ordinary differential equations.

The Source Iteration (SI) solution method decouples the S_N equations by lagging the right hand side of Eq. 4. In other words,

$$\mu_n\frac{\mathrm{d}\psi_n^{\ell+1}}{\mathrm{d}x}(x)+\Sigma_t(x)\psi_n^{\ell+1}(x)=\frac{\Sigma_s(x)}{2}\phi^{\ell}(x)+\frac{Q(x)}{2},\ 1\le n\le N \tag{4}$$

where $\psi_n^\ell(x)$ is the solution from the ℓ^{th} iteration. Equation 4 represents N independent ordinary differential equations. The iteration process begins with an initial guess for the scalar flux, $\phi^0(x)$. Equation 4 is then solved, using $\phi^0(x)$ on the right hand side, for the $\psi_n^1(x)$. $\phi^1(x)$ is then computed using Eq. 2. This process is repeated until

$$\frac{\|\phi^{\ell+1}(x) - \phi^\ell(x)\|}{\|\phi^{\ell+1}(x)\|} < \epsilon \tag{5}$$

where ϵ is a sufficiently small tolerance.

If $\phi^0(x) = 0$, then $\phi^\ell(x)$ is the scalar flux of particles that have undergone at most $\ell - 1$ collisions [1]. Thus, the number of iterations until convergence is directly linked to the number of collisions in a particle's lifetime. Typically, SI becomes increasingly slow to converge as the ratio of Σ_s to Σ_t approaches unity and the amount of particle leakage from the system goes to zero. SI is slowest in large, optically thick systems with small losses to absorption. In full radiation transport simulations each iteration could involve solving for hundreds of millions of unknowns. To minimize computational expense, acceleration schemes must be developed to rapidly increase the rate of convergence of SI.

Fortunately, the regime where SI is slow to converge is also the regime where Diffusion Theory is most accurate. A popular method for accelerating SI is Diffusion Synthetic Acceleration (DSA) where each source iteration involves both a transport sweep and a diffusion solve. DSA requires carefully differencing the S_N and diffusion steps in a consistent manner to prevent instability in highly scattering media with coarse spatial grids [4, 5]. DSA is not applicable in the setting of this presentation due to the incompatibility of MHFEM and S_N and the increased computational expense of solving consistently differenced diffusion. A new acceleration method is needed that avoids the consistency pitfall of DSA.

Eddington Acceleration

The first and second angular moments of Eq. 1 are

$$\frac{\mathrm{d}}{\mathrm{d}x} J(x) + \Sigma_a(x)\phi(x) = Q(x) \tag{6a}$$

$$\frac{\mathrm{d}}{\mathrm{d}x} \langle \mu^2 \rangle(x)\phi(x) + \Sigma_t(x) J(x) = 0 \tag{6b}$$

where $J(x) = \int_{-1}^{1} \mu\ \psi(x,\mu)\,\mathrm{d}\mu$ is the current and

$$\langle \mu^2 \rangle(x) = \frac{\int_{-1}^{1} \mu^2 \psi(x,\mu)\,\mathrm{d}\mu}{\int_{-1}^{1} \psi(x,\mu)\,\mathrm{d}\mu} \tag{7}$$

the Eddington factor. In S_N, the Eddington factor is

$$\langle \mu^2 \rangle(x) = \frac{\sum_{n=1}^{N} \mu_n^2 w_n \psi_n(x)}{\sum_{n=1}^{N} w_n \psi_n(x)}. \tag{8}$$

Note that no approximations have been made to arrive at Eqs. 6a and 6b. The Eddington factor is the true angular flux weighted average of μ^2 and therefore Eqs. 6a and 6b are just as accurate as Eq. 1.

This formulation is beneficial because Eq. 6a is a conservative balance equation and—if $\langle\mu^2\rangle(x)$ is known—the moment equations' system of two first–order, ordinary differential equations can be solved directly with well–established methods. However, computing $\langle\mu^2\rangle(x)$ requires already knowing the angular flux.

The proposed acceleration scheme is:

1) Compute $\psi_n(x)$ with S_N and an arbitrary spatial discretization
2) Compute $\langle\mu^2\rangle(x)$ with Eq. 8
3) Interpolate $\langle\mu^2\rangle(x)$ onto the MHFEM grid
4) Solve the moment equations for $\phi(x)$ with the preconditioned $\langle\mu^2\rangle(x)$ using MHFEM.

This process is one source iteration consisting of an S_N transport step to compute the Eddington factor and an MHFEM acceleration step to compute $\phi(x)$. The scalar flux from the acceleration step is used in the right hand side of Eq. 4 and steps 1–4 are repeated until the acceleration step's $\phi(x)$ converges according to Eq. 5.

Acceleration occurs because the Eddington factor is a weak function of angular flux. This means that even poor angular flux solutions can accurately approximate the Eddington factor. In addition, the moment equations model the contributions of all scattering events at once, reducing the dependence on source iterations to introduce scattering information. The solution from the acceleration step is then an approximation for the full flux and not the $\ell - 1$ collided flux as it was without acceleration.

In addition to acceleration, this scheme allows the S_N equations and moment equations to be solved with different spatial discretizations. S_N can be spatially discretized using normal methods such as Diamond Difference (DD) or Linear Discontinuous Galerkin (LD) while the moment equations can be solved on the same grid as the hydrodynamics.

Transport Step

Diamond Difference Discrete Ordinates

The DD S_N equations corresponding to Eq. 3 are

$$\frac{\mu_n}{h_i}\left(\psi_{n,i+1/2} - \psi_{n,i-1/2}\right) + \Sigma_{t,i}\psi_{n,i} = \frac{\Sigma_{s,i}}{2}\sum_{n'=1}^{N}\psi_{n',i}w_{n'} + \frac{Q_i}{2},\ 1 \le n \le N,\ 1 \le i \le I \tag{9}$$

where $\psi_{n,i\pm1/2} = \psi_n(x_{i\pm1/2})$ is the cell edge angular flux and $\Sigma_{t,i} = \Sigma_t(x_i)$, $\Sigma_{s,i} = \Sigma_s(x_i)$ and $Q_i = Q(x_i)$ the cell averaged total cross section, scattering cross section and fixed source. The $x_{i\pm1/2}$ are the cell edge locations of cell i of cell width $h = x_{i+1/2} - x_{i-1/2}$. In DD, the cell centered angular flux is taken to be the average of the adjacent cell edge angular fluxes:

$$\psi_{n,i} = \frac{1}{2}\left(\psi_{n,i+1/2} + \psi_{n,i-1/2}\right). \tag{10}$$

Using this result for the scattering term yields

$$\begin{aligned}\frac{\Sigma_{s,i}}{2}\sum_{n'=1}^{N}\psi_{n',i}w_{n'} &= \frac{\Sigma_{s,i}}{2}\sum_{n'=1}^{N}\frac{1}{2}\left(\psi_{n,i+1/2} + \psi_{n,i-1/2}\right)w_{n'} \\ &= \frac{\Sigma_{s,i}}{4}\left(\phi_{i-1/2} + \phi_{i+1/2}\right)\end{aligned} \tag{11}$$

In SI, the scattering term is lagged:

$$\frac{\mu_n}{h_i}\left(\psi^{\ell+1}_{n,i+1/2}-\psi^{\ell+1}_{n,i-1/2}\right)+\Sigma_{t,i}\psi^{\ell+1}_{n,i}=\frac{\Sigma_{s,i}}{4}\left(\phi^{\ell}_{i-1/2}+\phi^{\ell}_{i+1/2}\right)+\frac{Q_i}{2},\ 1\leq n\leq N,\ 1\leq i\leq I \quad (12)$$

Solving for $\psi^{\ell+1}_{n,j\pm1/2}$ yields

$$\psi^{\ell+1}_{n,i+1/2}=\frac{\frac{\Sigma_s}{2}h_i\left(\phi^{\ell}_{i-1/2}+\phi^{\ell}_{i+1/2}\right)+Q_ih_i-\left(\Sigma_th_i-2\mu_n\right)\psi^{\ell+1}_{n,i-1/2}}{\Sigma_th_i+2\mu_n},\ \mu_n>0 \quad (13a)$$

$$\psi^{\ell+1}_{n,i-1/2}=\frac{\frac{\Sigma_s}{2}h_i\left(\phi^{\ell}_{i-1/2}+\phi^{\ell}_{i+1/2}\right)+Q_ih_i-\left(\Sigma_th_i-2|\mu_n|\right)\psi^{\ell+1}_{n,i+1/2}}{\Sigma_th_i+2|\mu_n|},\ \mu_n<0 \quad (13b)$$

Equation 13a specifies the flux exiting the right side of cell i given the flux that entered through the left side while Eq. 13b specifies the flux exiting the left side of cell i given the flux that entered through the right side.

By specifying boundary conditions for $\psi^{\ell+1}_{n,1/2}$ for $\mu_n>0$ and $\psi^{\ell+1}_{n,I+1/2}$ for $\mu<0$, Eqs. 13a and 13b can be solved non-iteratively. The boundary conditions for a vacuum left boundary and reflecting right boundary are

$$\psi^{\ell+1}_{n,1/2}=0,\ \mu_n>0 \quad (14a)$$

$$\psi^{\ell+1}_{n,I+1/2}=\psi^{\ell+1}_{m,I+1/2},\ \mu_n=-\mu_m. \quad (14b)$$

Using Eq. 14a, the flux exiting the right side of cell $i=1$, $\psi^{\ell+1}_{n,3/2}$, can be found through Eq. 13a. This exiting flux is then the flux entering cell $i=2$ allowing for the determination of $\psi^{\ell+1}_{n,5/2}$. This process of using the result from the previous cell is repeated until $i=I$. At this point all rightward ($\mu>0$) moving flux has been determined for all cells $1\leq i\leq I$.

The reflecting boundary condition, Eq. 14b, can now be applied. This sets the incoming flux on the right side of cell $i=I$. Equation 13b then determines the exiting flux through the left side, $\psi^{\ell+1}_{n,I-1/2}$. Working backward from cell $i=I$, $\psi^{\ell+1}_{n,I-3/2},\psi_{n,I-5/2},\ldots,\psi^{\ell+1}_{n,1/2}$ for $\mu_n<0$ can be found. This process of propagating the solution from left to right for $\mu_n>0$ and then from right to left for $\mu_n<0$ is known as a transport sweep. At the end of the sweep, new cell edge scalar flux values $\phi^{\ell+1}_{i\pm1/2}$ are generated through

$$\phi^{\ell+1}_{i\pm1/2}=\sum_{n=1}^{N}\psi^{\ell+1}_{n,i\pm1/2}w_n. \quad (15)$$

A new sweep is then conducted using $\phi^{\ell+1}_{i\pm1/2}$. This process is repeated until the stop criterion of

$$\frac{\sum_{i=0}^{I}\left(\phi^{\ell+1}_{i+1/2}-\phi^{\ell}_{i+1/2}\right)^2}{\sum_{i=0}^{I}\left(\phi^{\ell+1}_{i+1/2}\right)^2}<\epsilon \quad (16)$$

is met.

Mixed Hybrid Finite Element Method Acceleration

The MHFEM as applied to Eqs. 6a and 6b uses the following basis functions:

$$B_{L,i}(x) = \begin{cases} \frac{x_{i+1/2}-x}{x_{i+1/2}-x_{i-1/2}}, \ x \in [x_{i-1/2}, x_{i+1/2}] \\ 0, \ \text{otherwise} \end{cases} \tag{17a}$$

$$B_{R,i}(x) = \begin{cases} \frac{x-x_{i-1/2}}{x_{i+1/2}-x_{i-1/2}}, \ x \in [x_{i-1/2}, x_{i+1/2}] \\ 0, \ \text{otherwise} \end{cases} . \tag{17b}$$

The scalar flux is constant within a cell with discontinuous jumps at the cell edges. In other words,

$$\phi_i(x) = \begin{cases} \phi_i, \ x \in (x_{i-1/2}, x_{i+1/2}) \\ \phi_{i\pm1/2}, x = x_{i\pm1/2} \\ 0, \ \text{otherwise} \end{cases} \tag{18}$$

with

$$\phi(x) = \sum_{i=1}^{I} \phi_i(x). \tag{19}$$

The Eddington factor will be interpolated onto the same grid as the scalar flux so that cell edge and cell center values will be available.

The current, $J(x)$, is a piecewise linear function defined by

$$J(x) = \sum_{i=1}^{I} J_{i,L} B_{L,i}(x) + J_{i,R} B_{R,i}(x) \tag{20}$$

where $J_{i,L}$ and $J_{i,R}$ are the current on the left and right edges of the cell.

Interior

On the interior cells, $i \in [2, I-1]$, each cell has five unknowns: $\phi_{i-1/2}$, ϕ_i, $\phi_{i+1/2}$, $J_{i,L}$, and $J_{i,R}$. Since $\phi_{i+1/2} = \phi_{(i+1)-1/2}$, only ϕ_i, $\phi_{i+1/2}$, $J_{i,L}$, and $J_{i,R}$ must be specified in each cell as the left edge of the cell is specified by the right edge of the previous cell. Thus four equations are needed for each interior cell.

The first is found by integrating Eq. 6a over cell i yielding the balance equation

$$J_{i,R} - J_{i,L} + \Sigma_{a,i}\phi_i h_i = Q_i h_i. \tag{21}$$

Equations for the cell edge current, $J_{i,L}$ and $J_{i,R}$, are found by multiplying Eq. 6b by $B_{L,i}(x)$ and $B_{R,i}(x)$ and integrating over cell i. This yields

$$\int_{x_{i-1/2}}^{x_{i+1/2}} B_{L,i}(x) \frac{\mathrm{d}}{\mathrm{d}x} \langle \mu^2 \rangle(x) \phi(x) + B_{L,i}(x) \Sigma_t(x) J(x) \, \mathrm{d}x = 0 \tag{22a}$$

$$\int_{x_{i-1/2}}^{x_{i+1/2}} B_{R,i}(x) \frac{\mathrm{d}}{\mathrm{d}x} \langle \mu^2 \rangle(x) \phi(x) + B_{R,i}(x) \Sigma_t(x) J(x) \, \mathrm{d}x = 0 \tag{22b}$$

Integrating by parts produces

$$-\langle\mu^2\rangle_{i-1/2}\phi_{i-1/2} + \langle\mu^2\rangle_i\phi_i + \Sigma_{t,i}h_i\left(\frac{J_{i,L}}{3} + \frac{J_{i,R}}{6}\right) = 0 \tag{23a}$$

$$\langle\mu^2\rangle_{i+1/2}\phi_{i+1/2} - \langle\mu^2\rangle_i\phi_i + \Sigma_{t,i}h_i\left(\frac{J_{i,L}}{6} + \frac{J_{i,R}}{3}\right) = 0. \tag{23b}$$

Eliminating $J_{i,L}$ from Eq. 23a and $J_{i,R}$ from Eq. 23b:

$$J_{i,R} = \frac{-2}{\Sigma_{t,i}h_i}\left[\langle\mu^2\rangle_{i-1/2}\phi_{i-1/2} - 3\langle\mu^2\rangle_i\phi_i + 2\langle\mu^2\rangle_{i+1/2}\phi_{i+1/2}\right] \tag{24}$$

$$J_{i,L} = \frac{-2}{\Sigma_{t,i}h_i}\left[-2\langle\mu^2\rangle_{i-1/2}\phi_{i-1/2} + 3\langle\mu^2\rangle_i\phi_i - \langle\mu^2\rangle_{i+1/2}\phi_{i+1/2}\right] \tag{25}$$

The equation for $\phi_{i+1/2}$ is found by enforcing continuity of current such that the current on the right side of cell i is equivalent to the current on the left side of cell $i+1$. In other words,

$$J_{i,R} = J_{i+1,L} \tag{26}$$

Applying this condition to Eqs. 24 and 25:

$$\begin{aligned}\frac{-2}{\Sigma_{t,i}h_i}\langle\mu^2\rangle_{i-1/2}\phi_{i-1/2} + \frac{6}{\Sigma_{t,i}h_i}\langle\mu^2\rangle_i\phi_i - 4\left(\frac{1}{\Sigma_{t,i}h_i} + \frac{1}{\Sigma_{t,i+1}h_{i+1}}\right)\langle\mu^2\rangle_{i+1/2}\phi_{i+1/2} \\ + \frac{6}{\Sigma_{t,i+1}h_{i+1}}\langle\mu^2\rangle_{i+1}\phi_{i+1} - \frac{2}{\Sigma_{t,i+1}h_{i+1}}\langle\mu^2\rangle_{i+3/2}\phi_{i+3/2} = 0.\end{aligned} \tag{27}$$

The required four equations can be reduced to two by replacing $J_{i,R}$ and $J_{i,L}$ in Eq. 21 with Eqs. 24 and 25. This produces the system of equations for every interior cell $i \in [2, I-1]$:

$$\phi_i = \frac{\frac{6}{\Sigma_{t,i}h_i}\langle\mu^2\rangle_{i-1/2}\phi_{i-1/2} + \frac{6}{\Sigma_{t,i}h_i}\langle\mu^2\rangle_{i+1/2}\phi_{i+1/2} + Q_ih_i}{\Sigma_{a,i}h_i + \frac{12}{\Sigma_{t,i}h_i}\langle\mu^2\rangle_i} \tag{28a}$$

$$\phi_{i+1/2} = \frac{\frac{-2}{\Sigma_{t,i}h_i}\langle\mu^2\rangle_{i-1/2}\phi_{i-1/2} + \frac{6}{\Sigma_{t,i}h_i}\langle\mu^2\rangle_i\phi_i + \frac{6}{\Sigma_{t,i+1}h_{i+1}}\langle\mu^2\rangle_{i+1}\phi_{i+1} - \frac{2}{\Sigma_{t,i+1}h_{i+1}}\langle\mu^2\rangle_{i+3/2}\phi_{i+3/2}}{4\left(\frac{1}{\Sigma_{t,i}h_i} + \frac{1}{\Sigma_{t,i+1}h_{i+1}}\right)\langle\mu^2\rangle_{i+1/2}} \tag{28b}$$

Boundary

Equation 28 provides $2(I-2)$ equations for the $2I+1$ unknowns. Thus, five boundary equations are required. The values not accounted for in Eq. 28 are $\phi_{1/2}$, ϕ_1, $\phi_{3/2}$, ϕ_I, and $\phi_{I+1/2}$.

The Marshak boundary condition is

$$\phi(x) + 2J(x) = 0. \tag{29}$$

At $x = x_{1/2}$:

$$\phi_{1/2} + 2J_{1,L} = 0 \tag{30}$$

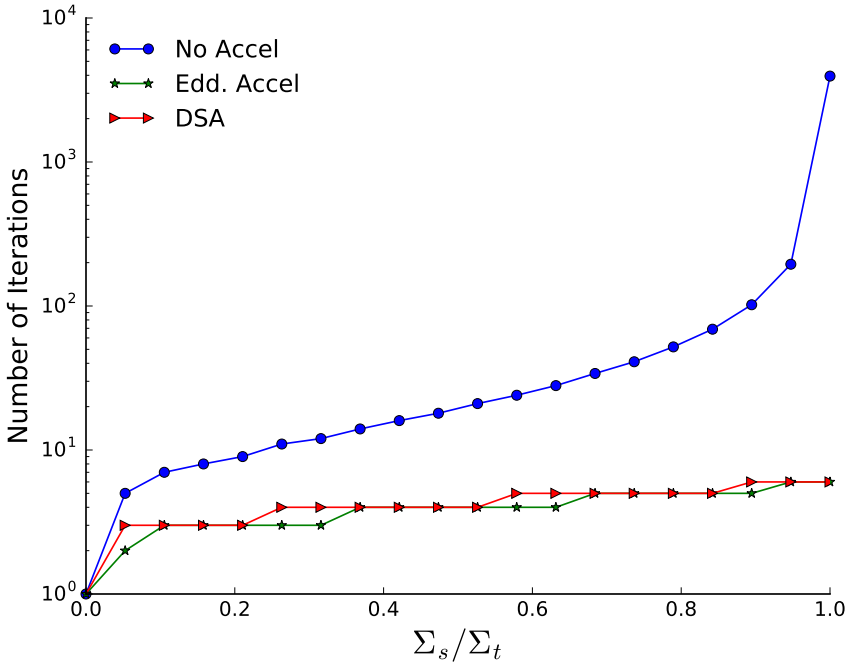

Fig. 1. A comparison of the number of iterations until convergence for unaccelerated, Eddington accelerated, and DSA S_8 SI.

Using Eq. 25 evaluated at $i = 1$,

$$\phi_{1/2} = \frac{\frac{6}{\Sigma_{t,i}h_i}\langle\mu^2\rangle_1\phi_1 - \frac{2}{\Sigma_{t,i}h_i}\langle\mu^2\rangle_{3/2}\phi_{3/2}}{\frac{1}{2} + \frac{4}{\Sigma_{t,i}h_i}\langle\mu^2\rangle_{1/2}} \tag{31}$$

Applying a reflecting boundary on the right edge $J(x_{I+1/2}) = J_{I,R} = 0$:

$$\phi_{I+1/2} = \frac{-\langle\mu^2\rangle_{I-1/2}\phi_{I-1/2} + 3\langle\mu^2\rangle_I\phi_I}{2\langle\mu^2\rangle_{i+1/2}} \tag{32}$$

ϕ_1 and ϕ_I are specified by Eq. 28a with $i = 1$ and $i = I$. The remaining unknown, $\phi_{3/2}$, is found through Eq. 28b with $i = 1$. There are now $2I + 1$ equations with $2I + 1$ unknowns. This system can be solved with the inversion of a banded matrix of bandwidth five.

Results

As a proof of concept for Eddington acceleration, a DD S_N code was created along with an MHFEM solver for Eqs. 6a and 6b. The test problem of steady–state, one–group, isotropically–scattering, fixed–source radiation transport in slab geometry with a reflecting left boundary and vacuum right boundary was used to compare unaccelerated, Eddington accelerated, and DSA S_8 SI with 100 spatial cells.

Figure 1 shows the number of iterations until the convergence criterion in Eq. 5 was met with $\epsilon = 1 \times 10^{-6}$ for varying ratios of Σ_s to Σ_t. Aside from $\Sigma_s/\Sigma_t = 0$ where acceleration is not possible, the ratio of unaccelerated to Eddington accelerated iterations ranges between 2.5 and 750. This

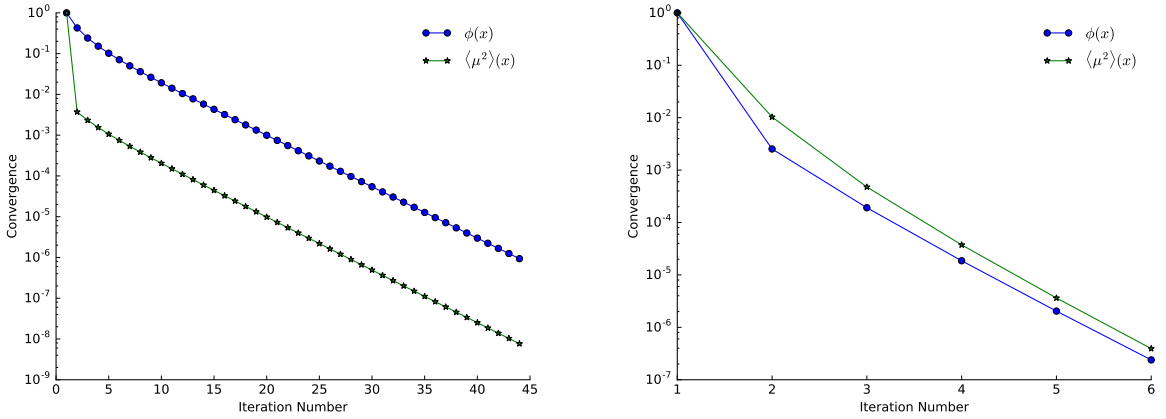

(a) (b)

Fig. 2. The convergence rate of $\phi(x)$ compared to $\langle\mu^2\rangle(x)$ for (a) unaccelerated and (b) Eddington accelerated S_8.

suggests that acceleration is occurring and that Eddington acceleration does not just do twice the amount of work in each iteration.

Figure 2a shows the unaccelerated convergence criterion

$$\frac{\|f^{\ell+1} - f^{\ell}\|}{\|f^{\ell+1}\|} \tag{33}$$

as a function of iteration number for $f = \phi(x)$ and $f = \langle\mu^2\rangle(x)$. The large drop in the convergence criterion between the first and second iterations supports the claim that $\langle\mu^2\rangle(x)$ is a weak function of angular flux as it quickly converges despite a less convergent angular flux. When compared to Fig. 2b, a plot of the convergence criterion versus number of iterations for Eddington accelerated S_8, it is clear that Eddington acceleration transfers the fast rate of convergence of $\langle\mu^2\rangle(x)$ to $\phi(x)$.

Conclusions

The proposed acceleration scheme successfully accelerated S_8 source iteration calculations in slab geometry for a wide range of Σ_s/Σ_t. In the pure scattering regime ($\Sigma_s = \Sigma_t$), source iteration was accelerated by a factor of 750. This scheme is especially suited for multiphysics applications because the transport and acceleration steps do not need to be consistently differenced. In addition, the acceleration step produces a conservative solution that is computationally inexpensive compared to a transport sweep. Future work that will also be presented is the application of Eddington acceleration to Linear Discontinuous Galerkin discretized S_N.

References

[1] M. L. ADAMS and E. W. LARSEN, *Fast Iterative Methods for Discrete–Ordinates Particle Transport Calculations*, vol. 40, Progress in Nuclear Technology (2002).

[2] F. BREZZI and M. FORTIN, *Mixed and Hybdrid Finite Element Methods*, Springer (1991).

[3] J. I. CASTOR, *Radiation Hydrodynamics* (2003).

[4] R. E. ALCOUFFE, *Diffusion Synthetic Acceleration Methods for the Diamond–Differenced Discrete–Ordinates Equations* (1977).

[5] J. S. WARSA, T. A. WAREING, and J. E. MOREL, *Fully Consistent Diffusion Synthetic Acceleration of Linear Discontinuous Transport Discretizations on Three–Dimensional Unstructured Meshes.*